Available online at www.sciencedirect.com

ScienceDirect

Ceramics International 40 (2014) 4277–4284

CERAMICS INTERNATIONAL

www.elsevier.com/locate/ceramint

Microstructure and dielectric properties of Dy/Mn doped $BaTiO_3$ ceramics

V. Paunovic[a,*], V.V. Mitic[a,b], Z. Prijic[a], Lj. Zivkovic[a]

[a]University of Nis, Faculty of Electronic Engineering, Aleksandra Medvedeva 14, 18000 Niš, Serbia
[b]Institute of Technical Sciences, SASA, Knez Mihailova 35, 11000 Belgrade, Serbia

Received 12 June 2013; received in revised form 21 August 2013; accepted 22 August 2013
Available online 31 August 2013

Abstract

Dy/Mn doped $BaTiO_3$ with different Dy_2O_3 contents, ranging from 0.1 to 5.0 at% Dy, were investigated regarding their microstructural and dielectric characteristics. The content of 0.05 at% Mn was constant in all the investigated samples. The samples were prepared by the conventional solid state reaction and sintered at 1290°, and 1350 °C in air atmosphere for 2 h. The low doped samples (0.1 and 0.5 at% Dy) exhibit mainly fairly uniform and homogeneous microstructure with average grain sizes ranged from 0.3 μm to 3.0 μm. At 1350 °C, the appearance of secondary, abnormal, grains in the fine grain matrix and core–shell structure were observed in highly doped Dy/$BaTiO_3$. Dielectric measurements were carried out as a function of temperature up to 180 °C. The low doped samples sintered at 1350 °C, display the high value of dielectric permittivity at room temperature, 5600 for 0.1Dy/$BaTiO_3$. A nearly flat permittivity–temperature response was obtained in specimens with 2.0 and 5.0 at% additive content. Using a Curie–Weiss and modified Curie–Weiss low, the Curie constant (C), Curie like constant (C'), Curie temperature (T_C) and a critical exponent (γ) were calculated. The obtained values of γ pointed out the diffuse phase transformation in highly doped $BaTiO_3$ samples.

Keywords: A. Sintering; B. Microstructures; C. Dielectric properties; D. $BaTiO_3$

1. Introduction

Rare earth oxides are widely used as doping materials for $BaTiO_3$ based multilayer capacitors [1–4]. The incorporation of trivalent rare-earth cations Dy^{3+}, Sm^{3+} and Ho^{3+}, which replaces predominately A sites in perovskite $BaTiO_3$ structure, modifies the microstructural and electrical properties of doped $BaTiO_3$. For lower donor concentration, up to 0.5 at%, named as grain growth inhibition threshold (GGIT), the bimodal microstructure is formed and anomalous grain growth occurred which leads to semiconductive properties of ceramics [5–9]. The substitution of Dy^{3+} on Ba^{2+} sites requires the formation of negatively charged defects. There are three possible compensation mechanisms: barium vacancies (V''_{Ba}), titanium vacancies (V''''_{Ti}) and electrons (e'). For samples sintered in air atmosphere, which are the electrical insulators, the principal doping mechanism is the ionic compensation mechanism. The controversy remains concerning whether the dominant ionic mechanism is through the creation of barium or titanium vacancies [10–13].

MnO_2 are frequently added to $BaTiO_3$ together with other additives in order to reduce the dissipation factor. In heavily, codoped $BaTiO_3$ ceramics, with small grained microstructure the resistivity is in the order of 10^{10} Ω cm. Manganese belongs to the valence unstable acceptor type dopant which may take different valence states, Mn^{2+}, Mn^{3+} or even Mn^{4+} during the post sintering annealing process. For codoped systems [14–16] the formation of donor–acceptor complexes such as $2[Dy^{\bullet}_{Ba}]$–$[Mn''_{Ti}]$ prevent a valence change from Mn^{2+} to Mn^{3+}.

The purpose of this paper is to study the microstructure and dielectric properties of Dy-doped $BaTiO_3$ in function of different amount of dopant concentration and sintering temperature. The Curie–Weiss and modified Curie–Weiss laws were used to clarify the influence of dopant on the dielectric properties of $BaTiO_3$.

*Corresponding author. Tel.: +381 18 529 325; fax: +381 18 588 399.
E-mail address: vesna.paunovic@elfak.ni.ac.rs (V. Paunovic).

0272-8842/$ - see front matter © 2013 Elsevier Ltd and Techna Group S.r.l. All rights reserved.
http://dx.doi.org/10.1016/j.ceramint.2013.08.092

2. Experimental procedure

The doped $BaTiO_3$ samples were prepared starting from reagent grade powders $BaTiO_3$, Rhone Poulenc (Ba/Ti= 0.996 ± 0.004, average particle size of 0.10–0.5 μm), and as additive Dy_2O_3 (Merck, Darmstadt). The content of additive oxides ranged from 0.1 to 5.0 at%. The content of MnO_2 (Merck, Darmstadt) was kept constant at 0.05 at% in all the samples. Raw materials were homogenized and ball milled in ethyl alcohol medium for 24h. The powders were milled by using polypropylene bottle and Al_2O_3 balls (10 mm balls diameter) as the milling media. After milling the slurries were dried in an oven at 200 °C for several hours until constant weigh and PVA was added as a binder. The dried powders were then pressed under a uniaxial pressure of 120 MPa into disk of 10 mm in diameter and 2 mm of thickness. The samples were sintered at 1290 °C and 1350 °C for 2 h in air atmosphere. The temperature regime during sintering was adjusted for 5 °C/min during heating and 10 °C/min during cooling in air atmosphere. The bulk density was measured by the Archimedes method. The specimens are denoted such as 0.1 Dy/BT for specimen with 0.1 at% Dy and 0.05 at% Mn and so on. The microstructures of the sintered or chemically etched samples were observed by scanning electron microscope JEOL-JSM 5300 equipped with EDS (QX 2000 S) system. X-ray diffraction (XRD) analyses were carried out by Rigaku-Miniflex diffractometer. Capacitance was measured by using HP 4276 LCZ meter in frequency range from 100 Hz to 20 kHz and the variation of dielectric constant with temperature was measured in a temperature interval from 20° to 180 °C.

3. Results and discussion

3.1. Microstructure characteristics

The relative density of Dy doped samples ranged from 78% of theoretical density (TD) for 0.1 Dy/BT samples sintered at 1290 °C to 90% TD for 0.1 Dy/BT samples sintered at 1350 °C. With increase of sintering temperature and decrease of additive content the density of investigated samples increase. The homogeneous and completely fine-grained microstructure, with grain size ranged from 0.5 to 3.0 μm, of fairly narrow size distribution, are the main characteristics of low doped ceramics, sintered at 1290 °C, as it is shown in Fig. 1a and b. With the increase of dopant amount, the increase of porosity is evident. For all samples the addition of Dy greatly inhibits the grain growth. At 1350 °C the microstructure for specimens with 0.1 and 0.5 at% Dy is similar to that, ones obtained for lower sintering temperature, as illustrated in Fig. 1c and d.

For higher content of additive, apart from the fine grained matrix, some local areas, with grains sized around 15 μm, were observed (Fig. 2a and b). Also, in grain size over 15 μm, the domain structure is detected (Fig. 2c). The domain width varies from 0.5 to 1 μm and the wall thickness is ranged from

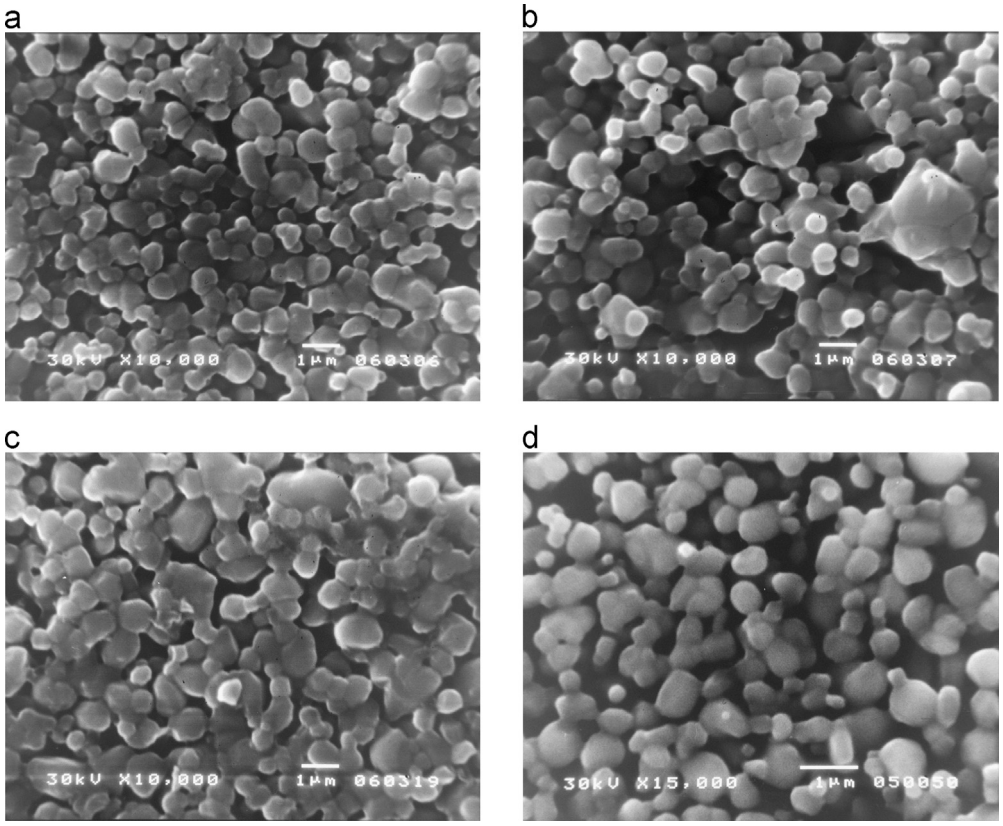

Fig. 1. SEM images of $Dy/BaTiO_3$, (a) 0.1 and (b) 0.5 at% Dy sintered at 1290 °C and (c) 0.1 and (d) 0.5 at% Dy sintered at 1350 °C.

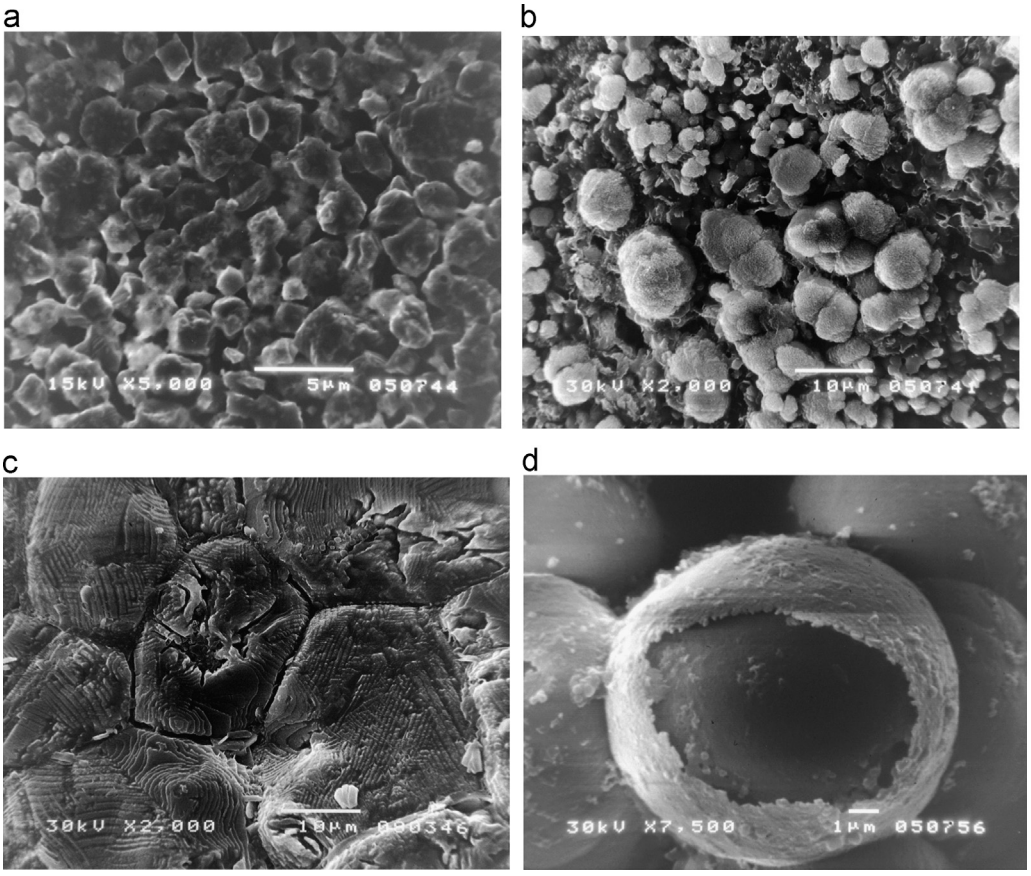

Fig. 2. SEM images of (a) 2.0 and (b) 5.0 at% doped Dy/$BaTiO_3$ sintered at 1350 °C. After chemical etching, (c) domain structure, and (d) core–shell structure.

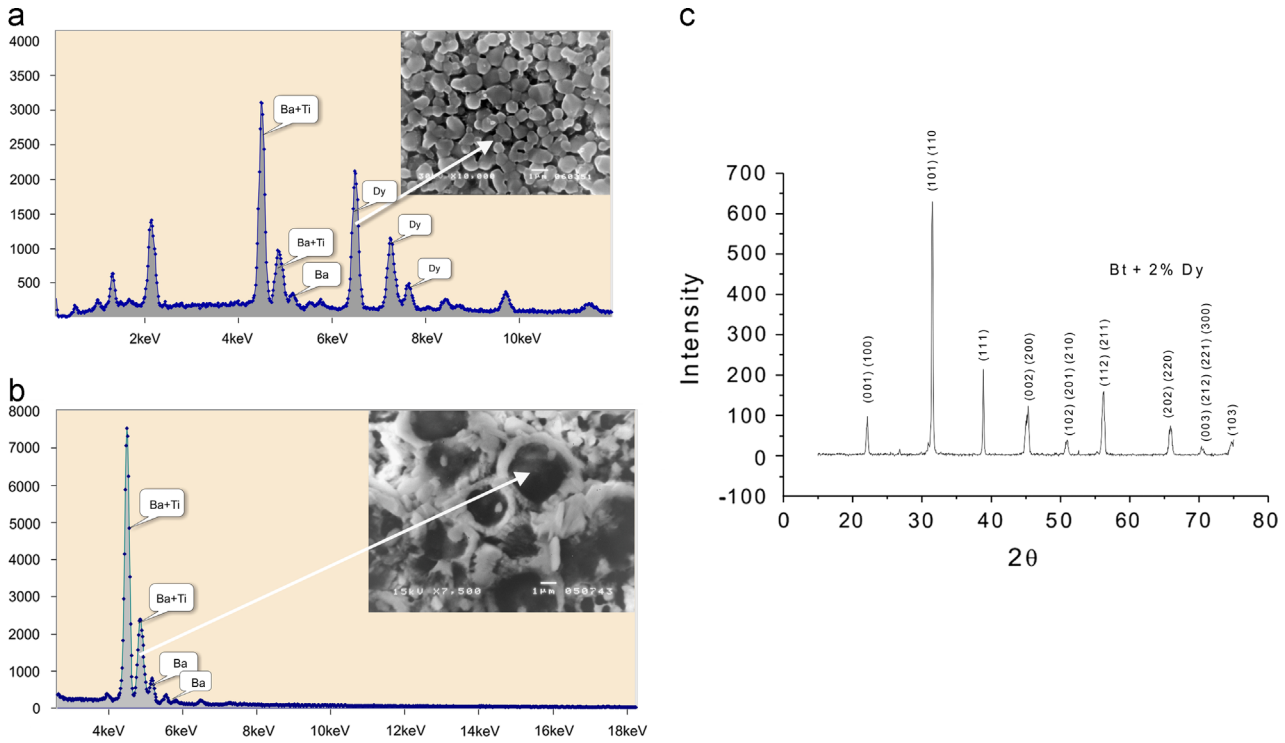

Fig. 3. SEM/EDS images of 2.0 Dy/BT sintered at 1350 °C, (a) fine-grained matrix rich in Dy and (b) regions with core–shell structure (core is free of Dy content), and (c) X-ray diffraction pattern for 2.0 Dy/$BaTiO_3$.

0.15 to 0.25 μm. After etching, the core–shell microstructure is evident in high doped samples, in 2.0 and 5.0 Dy/BT samples, Fig. 2d. The grain core indicates the un-doped ferroelectric region and the grain shell is the outer region, having a dopant gradient concentration towards the grain core. The average dielectric constant is the sum of dielectric constant of core and shell. Since the dopant is not homogeneously dispersed in $BaTiO_3$, the quantity of "core–shell" grains is limited.

The difference in microstructure features in highly doped samples is also associated with the inhomogeneous distribution of Dy_2O_3, as can be seen in EDS spectra, (Fig. 3), taken from different area in the same sample. According to the qualitative EDS analysis the Dy-rich regions are associated with small grained regions, as given in Fig. 3a, whereas EDS spectra free of Dy-content, corresponded to the large grains regions and grain core regions (Fig. 3b). The XRD pattern shows a crystalline phase which is consistent with a perovskite type structure (Fig. 3c). There is no evidence of any secondary phases.

3.2. Electrical characteristics

All investigated samples are electrical insulators with an electrical resistivity $\rho > 10^{10}\ \Omega$ cm at room temperature. The ionic compensation mechanism is exclusively involved and due to immobility of cation vacancies, at room temperature, the doped samples remain insulating. Also, in small grained microstructure, the thickness of grain boundary insulating layer becomes comparable to the size of grains and therefore the resistivity is very high [5]. In addition, the effective carrier's density is reduced due to the presence of Mn-acceptor.

The dielectric properties evaluation has been made by capacitance (dielectric permittivity) measurements in the frequency range from 100 Hz to 20 kHz. After a slight higher value of ε_r at low frequency, permittivity becomes nearly constant at frequency greater than 5 kHz (Fig. 4).

The dielectric constant of the investigated samples at room temperature ranged from 900 to 2200 for samples sintered at 1290 °C and from 1350 to 5600 for samples sintered at

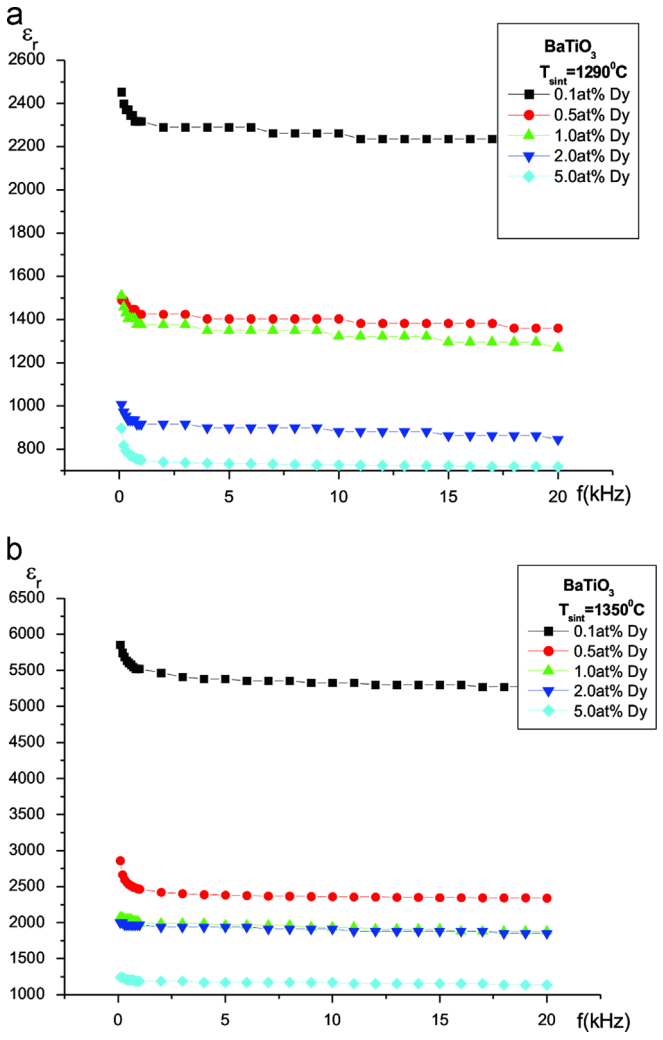

Fig. 4. Dielectric constant of Dy/$BaTiO_3$ ceramics in function of frequency (a) T_{sin} = 1290 °C, and (b) T_{sin} = 1350 °C.

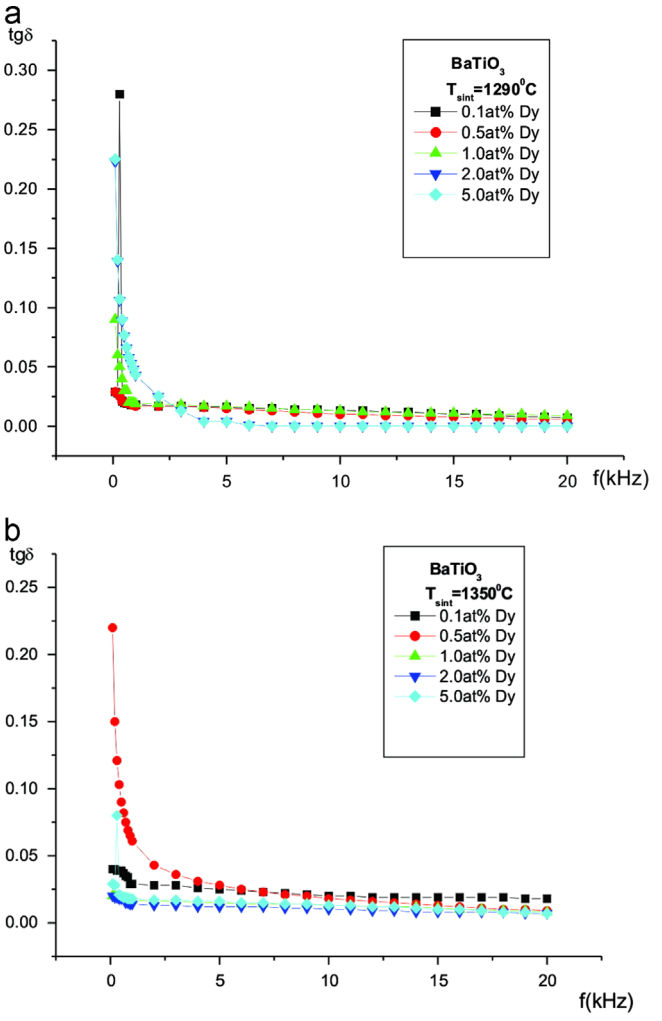

Fig. 5. The dissipation losses of Dy/$BaTiO_3$ ceramics sintered at (a) 1290 °C, and (b) 1350 °C in function of frequency.

1350 °C (Fig. 4). The highest value of permittivity at room temperature (ε_r=5600), and an evident dependence of frequency is recorded for 0.1 Dy/Mn–$BaTiO_3$ doped ceramics sintered at 1350 °C which is characterized by a uniform microstructure and highest density. With dopant content increase the dielectric constant decrease for both sintering temperature and for samples doped with 5.0 at% of Dy and sintered at 1290 °C the dielectric constant is 900, and for samples sintered at 1350 °C the dielectric constant is 1350.

The dissipation losses (Fig. 5), for all investigated samples, decrease with increase of frequency and sintering temperature. The corresponding curve for this sample could be separated into two regions with a change in linearity for frequency greater than 10 kHz. The loss tangents values (tan δ) were in the range from 0.03 to 0.28 for samples sintered at 1290 °C and from 0.02 to 0.22 for samples sintered at 1350 °C.

The influence of additives content on the dielectric behavior of modified $BaTiO_3$, can be analyzed through permittivity–temperature dependence given in Fig. 6. The variation in dielectric permittivity behavior can be related hardly only to the differences in microstructure, since the grain sizes are similar in most of the specimens. The observed variation in permittivity could be associated with the porosity and non-uniform compositional structure throughout the samples. A significant difference was observed in dielectric behavior between low and heavily doped samples.

The dielectric constant values increase with the increase of sintering temperature and decrease with additive content increase. Among the investigated Dy-doped samples, the highest value of dielectric permittivity of ε_r=5600, at room temperature and the greatest change at Curie temperature (ε_r=9130) were measured in 0.1 Dy/BT sintered at 1350 °C (Fig. 6).

The pronounced permittivity–temperature response and a sharp phase transition, from ferroelectric to paraelectric phase at Curie temperature (T_C), are observed for low doped samples with a small grained microstructure and high density. A small variation in dielectric permittivity at room and Curie tempera-

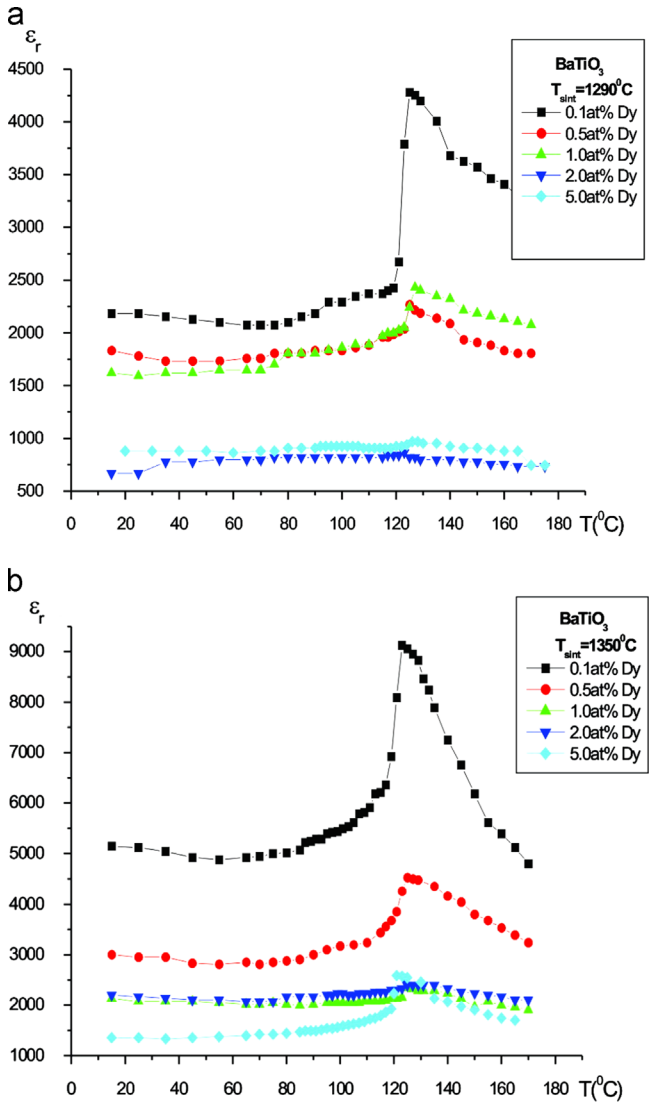

Fig. 6. Dielectric constant of doped $BaTiO_3$ sintered at (a) 1290 °C, and (b) 1350 °C in function of temperature.

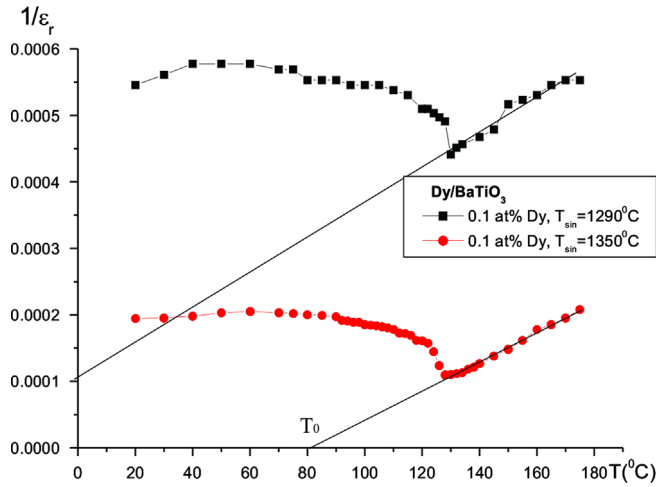

Fig. 7. Reciprocal value of ε_r in function of temperature for Dy doped $BaTiO_3$.

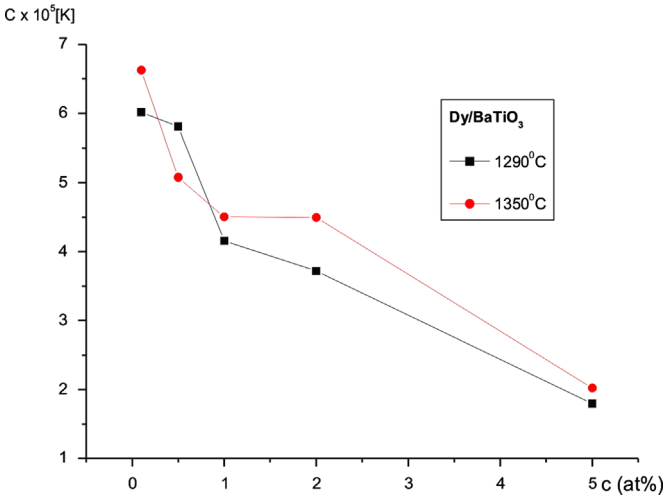

Fig. 8. Curie constant in function of additive content for doped $BaTiO_3$ samples.

Table 1
Dielectric parameters for Dy-doped $BaTiO_3$ sintered at 1290 °C.

Dy_2O_3 [at%]	T_{sin} = 1290 °C						
	ε_r ($T_{300\,K}$)	ε_r (T_C)	T_C [°C]	T_0 [°C]	$C \times 10^5$ [K]	$C^{/} \times 10^5$ [K]	γ
0.1	2200	4300	124	−35	6.61	1.30	1.01
0.5	1850	2300	125	−5	5.80	1.38	1.02
1.0	1620	2450	125	−117	4.15	1.96	1.02
2.0	870	900	126	−120	3.71	15.5	1.32
5.0	900	970	126	−55	1.79	16.5	1.40

Table 2
Dielectric parameters for Dy-doped $BaTiO_3$ sintered at 1350 °C.

Dy_2O_3 [at%]	T_{sin} = 1350°C						
	ε_r ($T_{300\,K}$)	ε_r (T_C)	T_C [°C]	T_0 [°C]	$C \times 10^5$ [K]	$C^{/} \times 10^5$ [K]	γ
0.1	5600	9130	123	82	6.62	4.85	1.02
0.5	3000	4530	124	−112	5.08	5.63	1.10
1.0	2130	2600	125	−62	4.55	8.54	1.41
2.0	2200	2500	125	21	4.49	25.1	1.43
5.0	1350	2650	126	48	2.02	56.8	1.71

ture and nearly flat and stable permittivity response of dielectric constant were observed for samples with higher dopant amount. The decrease in dielectric constant in doped samples with the increase of dopant concentration can be attributed on the one hand to the observed inhomogeneous distribution of additive throughout the specimens and on the other to the domain microstructure and core–shell grain configuration.

From the permittivity–temperature measurements Curie temperature was in the range of 123–126 °C being lower for low Dy doped $BaTiO_3$.

The dielectric constant for all specimens can be characterized by Curie–Weiss law, $\varepsilon_r = C/(T-T_0)$, which was used to calculate the dielectric parameters such as Curie constant (C) and Curie–Weiss temperature (T_0).

The Curie–Weiss temperature (T_0) was obtained from the linear extrapolation of the inverse dielectric constant from temperature above T_C down to zero (Fig. 7). The Curie constant (C) was obtained by fitting the plot of inverse values of dielectric constant vs. temperature and represents the slope of this curve for data above T_C.

The Curie constant (C) decreases with the increase of additive amount (Fig. 8), from $6.61 \cdot 10^5$ for 0.1 at% Dy to $1.79 \cdot 10^5$ for 5.0 at% Dy/$BaTiO_3$ samples sintered at 1290 °C and from $6.62 \cdot 10^5$ to $2.02 \cdot 10^5$ for 0.1 at% and 5.0 at% Dy/$BaTiO_3$ samples sintered at 1350 °C. In low doped samples, that exhibit a high density, the Curie constant is higher compared to the high doped samples. The value of Curie constant is related to the grain size and porosity of samples.

In order to investigate the Curie Weiss behavior, the modified Curie–Weiss law was used [17]

$$1/\varepsilon_r = 1/\varepsilon_{rmax} + (T-T_{max})^{\gamma}/C^{/} \quad (1)$$

where ε_r is dielectric constant, ε_{rmax} maximum value of dielectric constant, T_{max} temperature where the dielectric value has its maximum, γ critical exponent for diffuse phase transformation (DPT) and $C^{/}$ the Curie–Weiss-like constant. The dielectric parameters for doped $BaTiO_3$, together with the values calculated according to modified Curie–Weiss law, are given in Tables 1 and 2.

The critical exponent γ was calculated from the best fit of the curves $\ln(1/\varepsilon_r - 1/\varepsilon_{rmax})$ vs. $\ln(T-T_{max})$ (Fig. 9). The critical exponent γ is in the range $1 \le \gamma \le 2$, 1 for a sharp phase transformation and 2 for diffuse phase transformation. For $BaTiO_3$ single crystal γ is 1.08 and gradually increases up to 2 for diffuse phase transformation in modified $BaTiO_3$. In our case the critical exponent γ is ranged from 1.01 for 0.1 at% Dy/$BaTiO_3$ to 1.71 for 5.0 at% Dy/$BaTiO_3$ samples (Fig. 10), increases with the increase of additive concentration pointed out a diffuse phase transformation for heavily doped samples.

4. Conclusion

The relative density of Dy-doped ceramics ranged from 78% to 90% of TD, and increases with increase of sintering temperature. The low doped samples main characteristic is the uniform and homogeneous microstructure, with grain size ranged from 0.3 to 3.0 μm. For samples with 2.0 at% and 5.0 at% of additive, the grains size over 15 μm display core–shell and domain structure. All samples, independent of sintering temperature, have a resistivity $> 10^{10}$ Ω cm at room temperature. The highest dielectric constant of 5600 at room temperature and greatest change at Curie temperature (ε_r = 9130) were measured in 0.1 at% Dy/$BaTiO_3$, sintered at 1350 °C. Curie temperature was in the narrow range from 123 °C to 126 °C. The pronounced permittivity–temperature

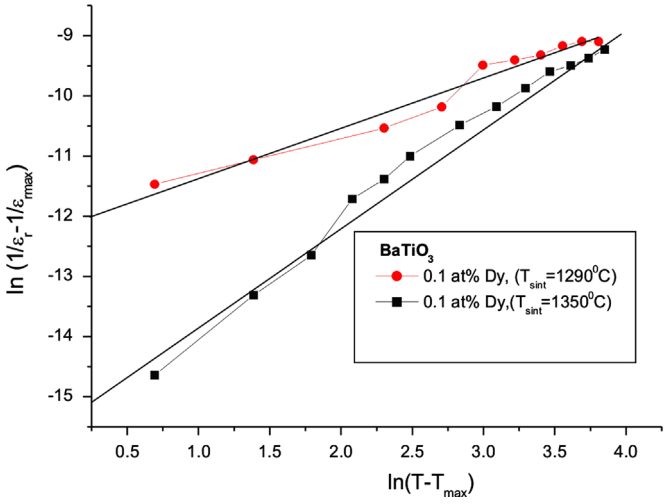

Fig. 9. The modified Curie–Weiss plot $\ln(1/\varepsilon_r - 1/\varepsilon_m)$ vs. $\ln(T-T_m)$ for selected $BaTiO_3$ samples. The slope of the curve determines the critical exponent γ.

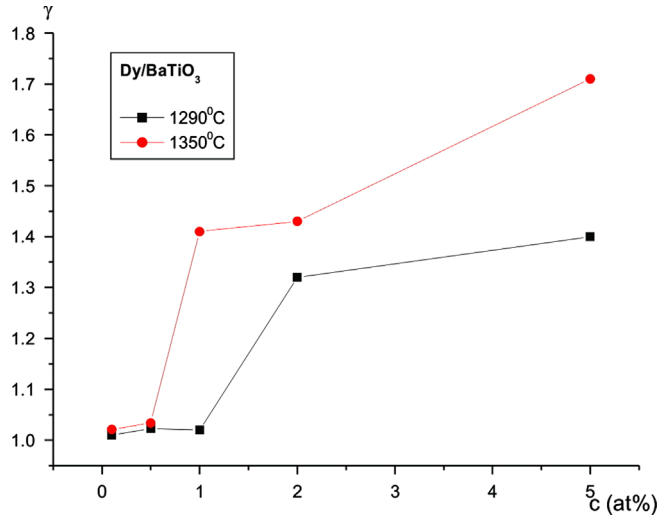

Fig. 10. The critical exponent γ for doped $BaTiO_3$ samples in function of additive concentration.

response and a sharp phase transition, from ferroelectric to paraelectric phase at Curie temperature, are observed for low doped samples with a small grained microstructure. The diffuse phase transformation characterized the heavily doped ceramics. A nearly flat and stable permittivity response was observed in specimens with 2.0 and 5.0 at% of dopant content. The differences of ε_r values in low and heavily doped barium titanate are due firstly, to the different porosity of doped ceramics and secondly, to the compositional inhomogeneous structure in heavily doped samples. The Curie constant decreases with the increase of additive amount from $6.62 \cdot 10^5$ to $2.02 \cdot 10^5$ for 0.1 at% and 5.0 at% $Dy/BaTiO_3$ samples. In low doped samples, that exhibit a high density and homogeneous microstructure, the Curie constant is higher compared to the high doped samples. The value of Curie constant is related to the grain size and porosity of samples. The critical exponent γ is ranged from 1.01 to 1.71 and increases with the increase of additive concentration. The obtained values of γ pointed out sharp phase transition for low doped specimens and diffuse phase transition for high doped specimens, which is in agreement with experimental results.

These analyses show that we can establish very precious control in prognosis and designing the specific dielectric properties within the Curie temperature area what is very important for new microstructure high level electronic circuits' integrations.

Acknowledgments

This research is part of the Project "Directed synthesis, structure and properties of multifunctional materials" (172057) and of the Project TR 32026. The authors gratefully acknowledge the financial support of Serbian Ministry of Education, Science and Technological Development for this work.

References

[1] H. Kishi, N. Kohzu, J. Sugino, H. Ohsato, Y. Iguchi, T. Okuda, The effect of rare-earth (La, Sm, Dy, Ho and Er) and Mg on the microstructure in $BaTiO_3$, Journal of the European Ceramic Society 19 (1999) 1043–1046.

[2] K.J. Park, C.H. Kim, Y.J. Yoon, S.M. Song, Y.T. Kim, K.H. Hur, Doping behaviors of dysprosium, yttrium and holmium in $BaTiO_3$ ceramics, Journal of the European Ceramic Society 29 (2009) 1735–1741.

[3] D.H. Kuo, C.H. Wang, W.P. Tsai, Donor and acceptor cosubstituted $BaTiO_3$ for nonreducible multilayer ceramic capacitors, Ceramics International 32 (2006) 1–5.

[4] V.V. Mitic, Z. Nikolic, V.B. Pavlovic, V. Paunovic, M. Miljkovic, B. Jordovic, L.j. Zivkovic, Influence of rare-earth dopants on barium titanate ceramics microstructure and corresponding electrical properties, Journal of the American Ceramic Society 93 (1) (2010) 132–137.

[5] W.H. Lee, W.A. Groen, H. Schreinemacher, D. Hennings, Dysporsium doped dielectric materials for sintering in reducing atmosphere, Journal of Electroceramics 5 (2000) 31–36.

[6] D. Makovec, Z. Samardžija, M. Drofenik, Solid solubility of Holmium, yttrium and dysprosium in $BaTiO_3$, Journal of the American Ceramic Society 87 (7) (2004) 1324–1329.

[7] V. Paunovic, L.j. Zivkovic, V. Mitic, Influence of rare-earth additives (La, Sm and Dy) on the microstructure and dielectric properties of doped BaTiO3 ceramics, Science of Sintering 42 (2010) 69–79.

[8] C. Pithan, D. Hennings, R. Waser, Progress in the synthesis of nanocrystalline $BaTiO_3$ powders for MLCC, International Journal of Applied Ceramic Technology 2 (1) (2005) 1–14.

[9] P. Kumar, S. Singh, J.K. Juneja, C. Prakash, K.K. Raina, Influence of calcium substitution on structural and electrical properties of substituted barium titanate 37 (2011) 1697–1700Ceramics International (2011) 1697–1700.

[10] R. Zhang, J.F. Li, D. Viehland, Effect of aliovalent substituents on the ferroelectric properties of modified barium titanate ceramics: Relaxor ferroelectric behavior, Journal of the American Ceramic Society 87 (2004) 864–870.

[11] F.D. Morrison, A.M. Coats, D.C. Sinclair, A.R. West, Charge compensation mechanisms in La-doped $BaTiO_3$, Journal of the European Ceramic Society (3) (2001) 219–2326 (3) (2001) 219–232.

[12] E.J. Lee, J. Jeong, Y.H. Han, Defects and degradation of $BaTiO_3$ codoped with Dy and Mn, Japanese Journal of Applied Physics 45 (2006) 822–825.

[13] S.M. Park, Y.H. Han, Dielectric relaxation of oxygen vacancies in Dy-doped $BaTiO_3$, Journal of the Korean Physical Society 57 (3) (2010) 458–463.

[14] H. Kishi, N. Kohzu, Y. Iguchi, J. Sugino, M. Kato, H. Ohasato, T. Okuda, Occupation sites and dielectric properties of rare-earth and Mn substituted $BaTiO_3$, Journal of the European Ceramic Society 21 (2001) 1643–1647.

[15] H. Miao, M. Dong, G. Tan, Y. Pu, Doping effects of Dy and Mg on $BaTiO_3$ ceramics preparedby hydrothermal method, Journal of Electroceramics 16 (2006) 297–300.

[16] K. Albertsen, D. Hennings, O. Steigelmann, Donor-acceptor charge complex formation in barium titanate ceramics: role of firing atmosphere, Journal of Electroceramics 2 (3) (1998) 193–198.

[17] K. Uchino, S. Namura, Critical exponents of the dielectric constants in diffuse-phase transition crystals, Ferroelectrics Letters 44 (1982) 55–61.